

and that when the Strutinsky method is used, the correction as suggested by KS is incorrect.

We acknowledge several useful discussions with Dr. R. K. Bhaduri, and one of the authors (C.S.W.) would like to thank Professor M. W. Johns for the hospitality of the Physics Department at McMaster University.

\*Work supported by the National Research Council of Canada.

†Permanent address: Tata Institute of Fundamental Research, Bombay 5, India.

<sup>1</sup>V. M. Strutinsky, Nucl. Phys. **A95**, 420 (1967).

<sup>2</sup>V. M. Strutinsky, Nucl. Phys. **A122**, 1 (1968).

<sup>3</sup>S. G. Nilsson, C. F. Tsang, A. Sobiczewski, Z. Szymanski, S. Wycech, C. Gustafson, I. L. Lamm, P. Mol-

ler, and B. Nilsson, Nucl. Phys. **A131**, 1 (1969).

<sup>4</sup>M. Brack, J. Damgaard, A. S. Jensen, H. C. Pauli, V. M. Strutinsky, and C. Y. Wong, Rev. Mod. Phys. **44**, 320 (1972).

<sup>5</sup>M. Bolsterli, E. O. Fiset, J. R. Nix, and J. L. Norton, Phys. Rev. C **3**, 1050 (1972).

<sup>6</sup>D. D. Clark, Phys. Today **24**, No. 12, 23 (1971).

<sup>7</sup>I. Kelson and Y. Shoshani, Phys. Lett. **40B**, 58 (1972).

<sup>8</sup>D. R. Inglis, Phys. Rev. **96**, 1059 (1954).

<sup>9</sup>H. J. Krappe and U. Wille, in *Proceedings of the Second International Atomic Energy Symposium on Physics and Chemistry of Fission, Vienna, Austria, 1969* (International Atomic Energy Agency, Vienna, 1969), p. 197.

<sup>10</sup>R. E. Peierls and J. Yoccoz, Proc. Phys. Soc., Sect. A **70**, 381 (1957); C. S. Warke and S. B. Khadkikar, Phys. Rev. **170**, 1041 (1968).

<sup>11</sup>A. Bohr, Kgl. Dan. Selsk., Mat.-Fys. Medd. **26**, No. 14 (1952).

## Nuclear Deformations from the Interference Effects between Coulomb and Nuclear Excitations in Inelastic $\alpha$ Scattering on $^{152}\text{Sm}$

W. Brückner, J. G. Merdinger,\* D. Pelte, U. Smilansky,† and K. Traxel

*Max-Planck-Institut für Kernphysik, and I. Physikalisches Institut der Universität Heidelberg, Heidelberg, Germany*

(Received 20 October 1972)

$\alpha$  particles in the energy range 11–18 MeV were used to excite the  $2^+$  and  $4^+$  members of the ground-state band in  $^{152}\text{Sm}$ . The measured excitation probabilities were analyzed in the framework of Coulomb excitation and the deformed optical model. The resulting electrical transition matrix elements and optical-model deformation parameters are  $\langle 0^+ \| m(E2) \| 2^+ \rangle = (1.86 \pm 0.03)e$  b,  $\langle 0^+ \| m(E4) \| 4^+ \rangle = (0.37 \pm 0.09)e$  b<sup>2</sup>,  $\beta_2 = 0.214 \pm 0.007$ , and  $\beta_4 = 0.038 \pm 0.007$ .

The hexadecapole deformations of the even-even isotopes in the rare-earth region were measured during the last few years by inelastic  $\alpha$  scattering.<sup>1-6</sup> The earliest experiments<sup>1,2</sup> used bombarding energies higher than the Coulomb barrier and the excitation interaction was considered to be mainly nuclear. The measured cross sections for the members of the ground band were analyzed in the framework of the deformed optical model. The deduced deformations are thus model dependent in two ways: (a) They depend on the validity of the assumption that the deformation parameters of the optical potential are related to the corresponding mass deformations, and (b) they assume that a simple rotational model holds rigorously for the lower members of the ground band. Later on, low-energy  $\alpha$  particles were used to Coulomb excite the  $4^+$  level in the ground band.<sup>3,4,6</sup> The single- $E4$  mode of excitation contributes about 10% of the total excitation cross section, while the re-

mainder is due to a double- $E2$  excitation process. From the measured  $E4$  transition matrix element  $\langle 0^+ \| m(E4) \| 4^+ \rangle$ , one can deduce the corresponding deformation parameter by assuming a functional form for the charge distribution, e.g., deformed Fermi distribution. The nuclear and charge deformation parameters thus obtained are in fair agreement. It seems, however, that the most sensitive way to study the connections between nuclear and charge deformation is the measurement of the interference between nuclear and Coulomb excitation. This has also the advantage that the parameters to be compared are determined under nearly the same conditions in one experiment.

In the experiment reported below, the elastic and inelastic cross sections were measured at energies between 11 and 18 MeV. In this energy range the low-energy data supply the matrix elements of the charge quadrupole and hexadecapole operators and the high-energy data determine

the optical-model deformation parameters  $\beta_2^N$  and  $\beta_4^N$ . The intermediate energies give information concerning the products of charge and mass deformations and enable the determination of their signs. The measurements were performed with the beam from the EN tandem Van de Graaff of the Max-Planck-Institut, Heidelberg, using  $^{152}\text{Sm}$  targets ( $20 \mu\text{g}/\text{cm}^2$ ) on thin carbon backings. The scattered particles were detected with Si detectors at  $170^\circ$ ,  $150^\circ$ ,  $130^\circ$ ,  $120^\circ$ ,  $100^\circ$ ,  $90^\circ$ , and  $70^\circ$  relative to both sides of the beam axis. Spectra were taken at intervals of 1 or sometimes 0.5 MeV. The energy resolution in these spectra, full width at half-maximum, was 20 keV.<sup>6</sup> The excitation probabilities  $R_I$  defined by  $R_I = (d\sigma/d\Omega)_I^{\text{inel}} / (d\sigma/d\Omega)_{\text{el}}$  were obtained from the various peak intensities which were extracted with the help of a computer code for line-shape analysis.<sup>7</sup> Elastic cross sections were measured as a function of the bombarding energy at  $\theta = 170^\circ$  and  $\theta = 150^\circ$ . They indicate that deviations from the prediction of the pure Coulomb law start at bombarding energies around 13 MeV. In the following we shall refer to the energy range below 13 MeV as the sub-Coulomb range.

The analysis of the sub-Coulomb data was carried out in the framework of Coulomb excitation.<sup>8</sup> It was observed by Alder *et al.*<sup>9</sup> that quantum-mechanical corrections are quite important for the extraction of the  $\langle 0^+ \| m(E4) \| 4^+ \rangle$  matrix element. We have therefore performed exact quantum-mechanical calculations by solving numerically the three-level coupled-channels problem. The contributions from virtual excitation of higher levels were calculated using the semiclassical Coulomb-excitation code.<sup>10</sup> The experimental results did not allow the matrix elements  $\langle 0^+ \| m(E2) \| 2^+ \rangle$  and  $\langle 2^+ \| m(E2) \| 4^+ \rangle$  to be determined independently. Instead, the measured lifetimes<sup>3</sup> of the  $2^+$  and  $4^+$  states were used to calculate the ratio  $\langle 2^+ \| m(E2) \| 4^+ \rangle / \langle 0^+ \| m(E2) \| 2^+ \rangle = 1.63 \pm 0.02$ . This ratio was kept constant throughout the analysis. The results for the charge-moment matrix elements are summarized in Ta-

ble I together with the results of other measurements. Our data are consistent with the more recent measurements which indicate that the  $E4$  matrix element obtained in Ref. 3 is too large. The charge-deformation parameters were calculated from the mean values of the  $\langle 0^+ \| m(E2) \| 2^+ \rangle$  and  $\langle 0^+ \| m(E4) \| 4^+ \rangle$  matrix elements assuming a deformed Fermi charge distribution. With a charge radius of  $6.09 \pm 0.015$  fm and a diffuseness of 0.5 fm suggested by muonic atoms,<sup>11</sup> the deformation parameters are  $\beta_4^C = 0.268 \pm 0.006$  and  $\beta_4^C = 0.058 \pm 0.012$ .

The analysis of the data from the higher energy range was performed in the framework of the deformed optical model. Our treatment of the problem followed the standard lines which are discussed in the literature.<sup>1,2</sup> Some points had to be given special attention: (a) The Coulomb interaction plays an important role in the energy domain under consideration. The long range of the  $E2$  component requires the integration of the differential equations to rather large distances ( $\sim 150$  fm), and also the inclusion of many (a few hundred) partial waves. The former requirement was met by choosing the Noumerov method<sup>12</sup> to integrate the coupled differential equations. The inclusion of the many partial waves was done following the method discussed in Samuel *et al.*<sup>13</sup> (b) The charge matrix elements were taken from the sub-Coulomb analysis. They were not varied together with  $\beta_2$  and  $\beta_4$ . The charge radius  $R_c = 7.5$  fm was used to determine which form of the Coulomb potential should be used depending on whether  $r < R_c$  or  $r > R_c$ .  $R_c$  also includes the contribution due to the  $\alpha$ -particle charge radius. (c) The optical potential was expanded in powers of the deformation parameters up to the fourth order. Comparison of third- and fourth-order calculations indicates that the convergence is rapid enough and justifies the use of the fourth-order expansion. The "spherical" optical-model parameters  $V_0$ ,  $W_0$ ,  $R_0$ , and  $a$  were taken from Ref. 2. In spite of the lower bombarding energies used in our experiment,

TABLE I. Transition matrix elements between the first three members of the ground band in  $^{152}\text{Sm}$ .

	This experiment	Coulomb excitation Ref. 3	Ref. 4	Ref. 14	Lifetime, Ref. 3	Electron scattering, Ref. 5
$\langle 0^+ \  m(E2) \  2^+ \rangle$ (e b)	$1.86 \pm 0.03$		$1.84 \pm 0.02$	$1.88 \pm 0.05$	$1.83 \pm 0.02$	
$\langle 0^+ \  m(E4) \  4^+ \rangle$ (e b <sup>2</sup> )	$0.37 \pm 0.09$	$0.45 \pm 0.09$	$0.35 \pm 0.07$			$0.37 \pm 0.02$

TABLE II. Optical-model parameters for the  $\alpha$  scattering on  $^{152}\text{Sm}$ .

	Bombarding energy (MeV)	$V_0$ (MeV)	$W_0$ (MeV)	$R_0$ (fm)	$a$ (fm)	$\beta_2^N$	$\beta_4^N$
This experiment	14–18	45.0	11.2	7.963	0.605	$0.214 \pm 0.007^a$	$0.038 \pm 0.007^a$
Ref. 2	27.5–32.5	50.0	11.2	7.963	0.605		
Ref. 1	50	65.9	27.3	7.685	0.637	0.205	0.040

<sup>a</sup>Errors corresponding to 1 standard deviation in  $\chi^2$  with respect to  $\beta_2^N$  and  $\beta_4^N$ .

we had to modify them only slightly (Table II) in order to fit our elastic scattering results. Most coupled-channels calculations were done by limiting the number of levels to 3. In some test cases the  $6^+$  level was also included, but only a minor change was observed. The  $\beta_6$  parameter was set equal to zero in all the calculations.

The experimental results together with the best-fitting theory are shown in Fig. 1. In order to emphasize the interference between the Coulomb and nuclear modes of excitation, we normalized the experimental and theoretical excitation probabilities by the prediction of the pure

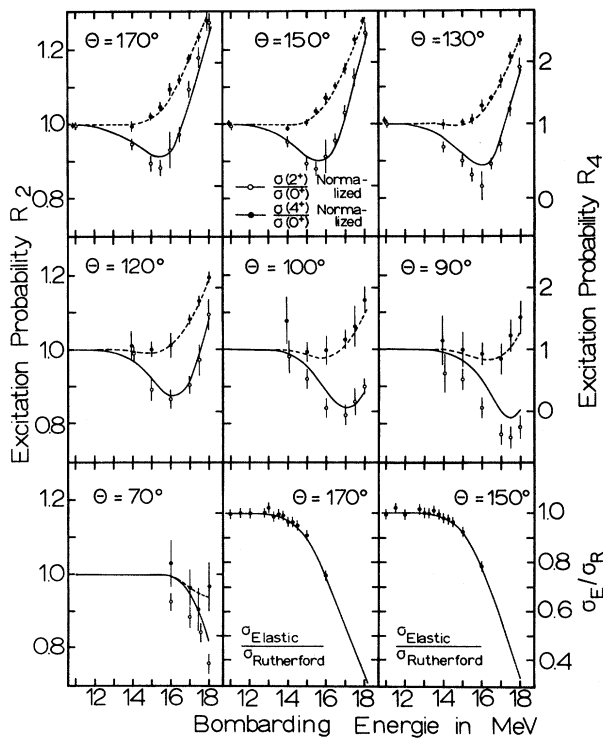


FIG. 1. Measured and calculated elastic cross sections and the excitation probabilities for the  $2^+$  and  $4^+$  levels. All results are normalized to the expectations of the pure Coulomb-excitation theory.

Coulomb-excitation theory. The  $2^+$  excitation probabilities show a very marked destructive interference between the nuclear and Coulomb contributions. The excitation probabilities decrease below the prediction of the pure Coulomb theory reaching a minimum whose depth and position depend on the scattering angle. Above a certain energy the nuclear amplitude dominates and the deviations from the Coulomb predictions increase very rapidly. The  $4^+$  excitation probabilities show almost no destructive interference pattern, and they seem to follow the predictions of the pure Coulomb theory even for those energies where  $R_2$  shows deviations. We believe that the behavior of  $R_2$  and  $R_4$  near the Coulomb barrier can be qualitatively explained in the following way. The destructive interference in the  $2^+$  excitation is due to the different signs of the nuclear and Coulomb interactions because the main contribution to the  $2^+$  excitation amplitude comes from first-order Coulomb and nuclear processes. The most important components in the excitation amplitude for the  $4^+$  state are (a) two-step processes due to either  $E2$  Coulomb or  $\lambda = 2$  nuclear excitations, (b) direct  $E4$  excitation, and (c) direct  $\lambda = 4$  nuclear excitation. The bulk of the cross section comes from the square of (a), while the processes (b) and (c) contribute to the cross section mainly through their interference with (a).

A series of excitation functions were calculated in which the signs of  $\beta_4^C$  and  $\beta_4^N$  were changed. The excitation probabilities  $R_4$  normalized by the pure Coulomb excitation are displayed in Fig. 2 for  $\theta = 170^\circ$ . The two signs shown as indices of  $R_4$  refer to the signs of  $\beta_4^C$  and  $\beta_4^N$ , respectively. Figure 2 clearly indicates that the interference between the various components in the scattering amplitude is quite important. A comparison between  $R_4^{++}$  and  $R_4^{--}$  shows that measuring the excitation function at backward angles is a very convenient tool to obtain the sign of the  $\lambda = 4$

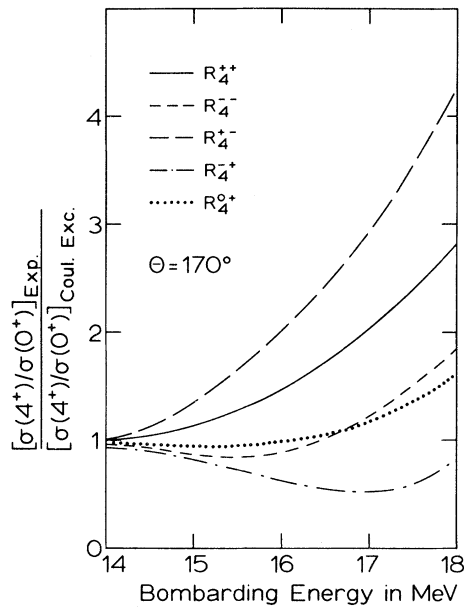


FIG. 2. Calculated excitation probabilities of the  $4^+$  level for various charge and optical-model deformations (see text). The results are normalized to the expectations of the pure Coulomb-excitation theory.

charge and optical-model deformation parameters. The pure Coulomb-excitation measurements are almost insensitive to the sign of  $\beta_4^C$  as indicated by the convergence of the various  $R_4$  functions at 14 MeV.

The  $\beta_2^N$  and  $\beta_4^N$  obtained in our measurement together with the results of Ref. 1 are given in Table II. These values are different from  $\beta_2^C$  and  $\beta_4^C$  since the radius parameters are unequal.

However, the products  $\beta_\lambda R$  should be equal<sup>1</sup> if the two sets of data are consistent. Using this criterion, the nuclear deformation parameters were calculated to be  $\beta_2^N = 0.279 \pm 0.009$  and  $\beta_4^N = 0.050 \pm 0.009$  for a radius parameter  $R = 6.093$  fm. These values are within the uncertainties in agreement with  $\beta_2^C$  and  $\beta_4^C$ .

\*On leave from the Centre de Recherches Nucléaires, Strasbourg, France.

†On leave from the Weizman Institute for Science, Rehovot, Israel.

<sup>1</sup>D. L. Hendrie *et al.*, Phys. Lett. **268**, 127 (1968).

<sup>2</sup>A. A. Aponick *et al.*, Nucl. Phys. **159A**, 267 (1970).

<sup>3</sup>F. S. Stephens *et al.*, Phys. Rev. Lett. **27**, 1151 (1971).

<sup>4</sup>T. K. Saylor *et al.*, to be published.

<sup>5</sup>W. Bertozzi *et al.*, Phys. Rev. Lett. **28**, 1711 (1972).

<sup>6</sup>W. Brückner *et al.*, in Proceedings of the Osaka Conference on Nuclear Moments, 1972 (to be published).

<sup>7</sup>G. Jansen, Ph. D. thesis, Heidelberg University, 1969 (unpublished).

<sup>8</sup>P. Winkler, Nucl. Phys. **168A**, 139 (1971).

<sup>9</sup>K. Alder *et al.*, Phys. Lett. **32B**, 645 (1970).

<sup>10</sup>A. Winther and J. de Boer, in *Coulomb Excitation*, edited by K. Alder and A. Winther (Academic, New York, 1966).

<sup>11</sup>S. Devons and I. Duerdoth, in *Advances in Nuclear Physics*, edited by M. Baranger and E. Vogt (Plenum, New York, 1969), Vol. 2.

<sup>12</sup>J. Raynal, Ph. D. thesis, Centre d'Etudes Nucléaires de Saclay Report No. DOC/68-3/DD (unpublished).

<sup>13</sup>M. Samuel *et al.*, Comput. Phys. Commun. **2**, 455 (1971).

<sup>14</sup>E. M. Bernstein *et al.*, Phys. Rev. **121**, 841 (1961).

## Higher-Order Correlation Properties of a Laser Beam\*

S. Chopra and L. Mandel

Department of Physics and Astronomy, University of Rochester, Rochester, New York 14627

(Received 9 November 1972)

The intrinsic third-order intensity correlation function of a laser beam has been measured by a digital correlation technique, for a He:Ne laser operating near threshold. The results are compared with some recent calculations of Cantrell, Lax, and Smith and are found to be in good agreement.

In recent years there has been considerable interest in the correlation properties of laser light, particularly when the laser is operating near its threshold of oscillation. However, with one exception,<sup>1</sup> all correlation measurements have been confined to the second-order intensity correlation function, and the higher-order correlation

properties have received little or no attention.<sup>2</sup> The reason is not hard to find. Correlation experiments of the third or higher order involve measurements of the arrival times of three or more photons, and require an order of magnitude more electronic data storage and analysis than the corresponding second-order problem. At the